Molecular Crystals and Liquid Crystals

ISSN: 1542-1406 (Print) 1563-5287 (Online) Journal homepage: http://www.tandfonline.com/loi/gmcl20

Localized Modes in Optics of Chiral Liquid Crystals

V. A. Belyakov

To cite this article: V. A. Belyakov (2015) Localized Modes in Optics of Chiral Liquid Crystals, Molecular Crystals and Liquid Crystals, 612:1, 81-97, DOI: 10.1080/15421406.2015.1030577

To link to this article: http://dx.doi.org/10.1080/15421406.2015.1030577

Published online: 06 Jul 2015.

Mol. Cryst. Liq. Cryst., Vol. 612: pp. 81–97, 2015

ISSN: 1542-1406 print/1563-5287 online
DOI: 10.1080/15421406.2015.1030577

Taylor & Francis
Taylor & Francis Group

Localized Modes in Optics of Chiral Liquid Crystals

V. A. BELYAKOV*

Landau Institute for Theoretical Physics, Moscow, Russia

The localized opical modes in photonic liquid crystals are studied for the certainty at the example of chiral liquid crystals (CLCs). The chosen here model (absence of dielectric interfaces in the studied structures) allows one to get rid off the polarization mixing at the surfaces of the CLC layer and the defect structure (DMS) and to reduce the corresponding equations to the equations for the light of diffracting in the CLC polarization only. The dispersion equations determining connection of the EM and DM frequencies with the CLC layer parameters and other parameters of the DMS are obtained. Analytic expressions for the transmission and reflection coefficients of the DMS are presented and analyzed. As specific cases are considered DMS with an active (i.e. transforming the light intensity or polarization) defect layer and CLC layers with locally anisotropic absorption. It is shown that the active layer (excluding an amplifying one) reduces the DM lifetime (and increase the lasing threshold) in comparison with the case of DM at an isotropic defect layer. The case of CLC layers with an anisotropic local absorption is also analyzed and, in particular, shown that due to the Borrmann effect the EM life-times for the EM frequncies at the opposite stop-bans edges may be signifinately different. The options of experimental observations of the theoretically revealed phenomena are discussed.

Keywords Chiral liquid crystals; edge and defect modes; low threshold lasing

1. Introduction

Recently there have been much activities in the field of localized optical modes, in particular, edge modes (EM) and defect modes (DM) in chiral liquid crystals (CLCs) mainly due to the possibilities to reach a low lasing threshold for the mirrorless distributed feedback (DFB) lasing [1–4] in CLCs. The EM and DM existing as a localized electromagnetic eigenstate with its frequency close to the forbidden band gap and in the forbidden band gap, respectively, were investigated initially in the periodic dielectric structures [5]. The corresponding EM and DM in CLCs, and more general in spiral media, are very similar to the EM and DM in one-dimensional scalar periodic structures. They reveal abnormal reflection and transmission [1, 2], and allow DFB lasing at a low lasing threshold [3].

Almost all studies of the EM and DM in chiral and scalar periodic media were performed by means of a numerical analysis with the exceptions [6, 7] where the known exact

*Address correspondence to V. A. Belyakov, Landau Institute for Theoretical Physics, 119334, Kosygin St. 2, Moscow, Russia. Email: bel@landau.ac.ru

Color versions of one or more of the figures in the article can be found online at www.tandfonline.com/gmcl.

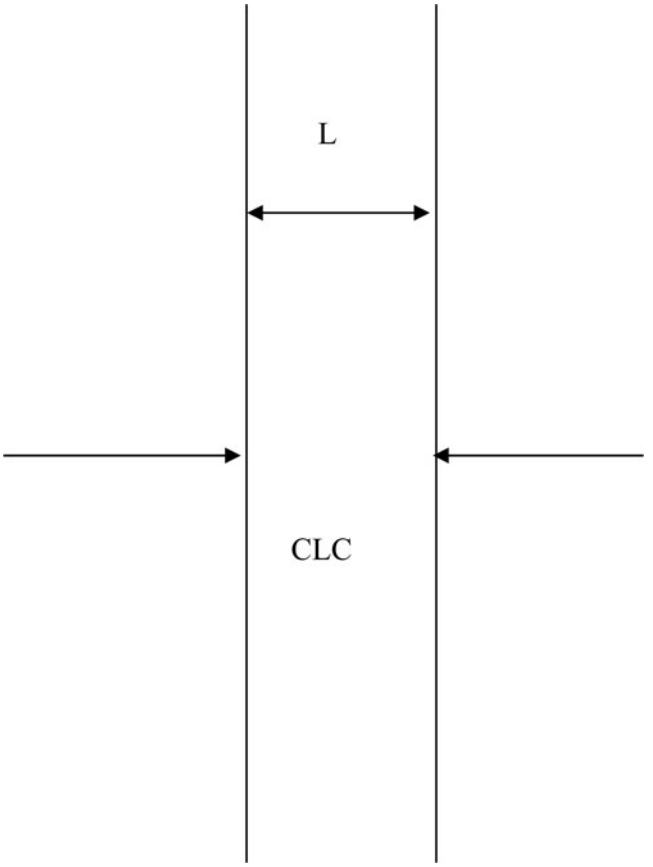

Figure 1. Schematic of the boundary problem for edge mode.

analytical expression for the eigenwaves propagating along the helix axis [8, 9] were used for a general study of the DM. The approach used in [6, 7] looks as fruitful one because it allows to reach easy understanding of the DM and EM physics, and this is why it deserves further implementation in the study of the EM and DM.

In the present work, analytical solutions of the EM and DM (associated with an insertion of a layer in the perfect cholesteric structure and CLCs with local anisotropy of absorption) are presented and some limiting cases simplifying the problem are considered.

2. The Boundary-Value Problem

To investigate EM in a CLC, we have to consider a boundary problem, i.e. transmission and reflection of light incident on a CLC layer along the spiral axis [10–12]. We assume that the CLC is represented by a planar layer with a spiral axis perpendicular to the layer surfaces (Figure 1). We also assume that the average CLC dielectric constant ε_0 coincides with the dielectric constant of the ambient medium. This assumption practically prevents conversion of one circular polarization into another at layer surfaces [11, 12], and allows to have only two eigenwaves with diffracting circular polarization taken into account.

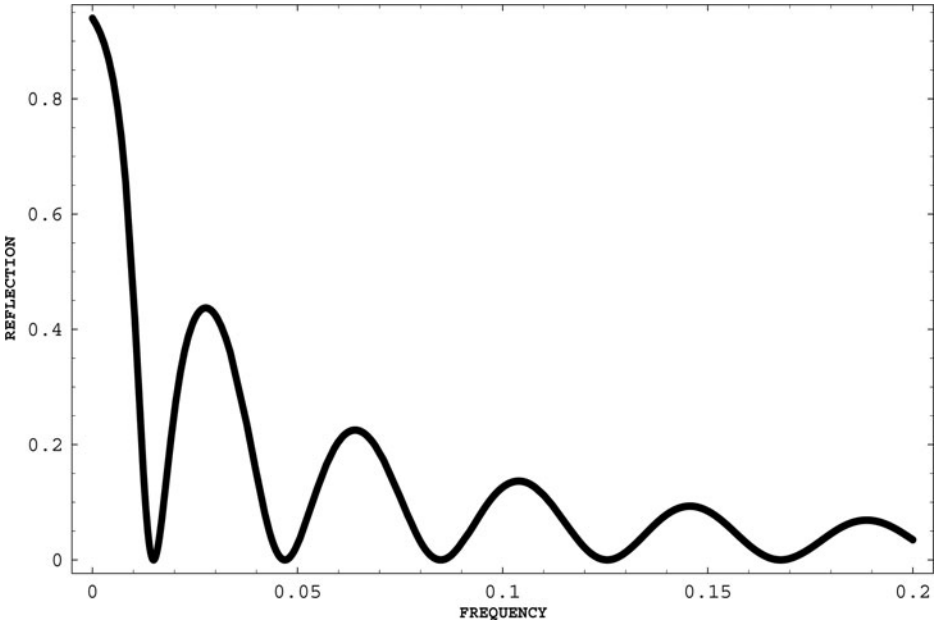

Figure 2. A typical intensity reflection coefficient for a nobabsorbing CLC layer calculated vs. the frequency, (shown close to one frequency edge of the stop band).

In the view of refs. [10–13], we state here only the final expressions for the amplitude transmission T and reflection R coefficients for light incident on a CLC layer of thickness L. These are given as

$$\mathrm{R(L)} = \delta \sin \mathrm{qL} / \left\{ (\mathrm{q}\tau/\kappa^2) \cos \mathrm{qL} + \mathrm{i}\left[(\tau/2\kappa)^2 + (\mathrm{q}/\kappa)^2 - 1 \right] \sin \mathrm{qL} \right\} \tag{1a}$$

$$\mathrm{T(L)} = \exp[\mathrm{i}\kappa \mathrm{L}](\mathrm{q}\tau/\kappa^2) / \left\{ (\mathrm{q}\tau/\kappa^2) \cos \mathrm{qL} + \mathrm{i}\left[(\tau/2k)^2 + (\mathrm{q}/\kappa)^2 - 1 \right] \sin \mathrm{qL} \right\}. \tag{1b}$$

where,

$$\mathrm{q} = \kappa \left\{ 1 + (\tau/2\kappa)^2 - [(\tau/\kappa)^2 + \delta^2]^{1/2} \right\}^{1/2} \text{ and, } \in_0 = (\varepsilon_\parallel + \varepsilon_\perp)/2, \delta = (\varepsilon_\parallel - \varepsilon_\perp)/(\varepsilon_\parallel - \varepsilon_\perp).$$

Here δ is the dielectric anisotropy with $\varepsilon_\parallel$ and $\varepsilon_\perp$ as the local principal values of the CLC dielectric tensor [10–12], $\kappa = \omega \in_0 / c$ with c as the speed of light, and $\tau = 4\pi/p$ with p as the cholesteric pitch.

Figure 2 demonstrates that the values of the reflection coefficient are strongly oscillating functions of the frequency close to the stop-band edges. The same is happening with the eigenwave amplitudes excited in the layer [13, 14]. At the points of maxima close to the stop-band edges, the eigenwave amplitudes are much larger than the incident wave amplitude. It turns out that the frequencies of the eigenwave amplitude

maxima coincide with the frequencies of zero reflection for a nonabsorbing CLC (see Figure 2).

3. Edge Mode (Non-Absorbing Liquid Crystal)

In a non-absorbing CLC, $\gamma = 0$ in the general expression for the dielectric constant $\varepsilon = e_0(1+i\gamma)$. The calculations of the reflection and transmission coefficients as functions of the frequency in accordance with Eqs. (1) (Figure 2) give the well-known results [8–12], in particular, $T+R = 1$ where the notations R and T here are the intensity reflection and transmission coefficients, respectevely for all frequencies.

The mentioned relation between the amplitudes of eigenwaves excited in the layer and incident waves at the specific frequencies shows that the energy of radiation in the CLC at the layer thickness for these frequencies is much higher than the corresponding energy of the incident wave at the same thickness.

Hence, in complete accordance with ref. [13], we conclude that at the corresponding frequencies, the incident wave excites some localized mode in the CLC. To find this localized mode, we have to solve the homogeneous system of linear equations [14].

The solvability condition for this homogeneous system determines the discrete frequencies of these localized modes:

$$\mathrm{tg}qL = \mathrm{i}\left(q\tau/\kappa^2\right) / \left[(\tau/2\kappa)^2 + (q/\kappa)^2 - 1\right] \tag{2}$$

Generally, solutions to Eq. (2) for the EM frequencies ω_{EM} can to be found only numerically. The EM frequencies ω_{EM} turn out to be complex, which can be presented as $\omega_{\mathrm{EM}} = \omega(1+\mathrm{i}\Delta)$ where Δ is a small parameter in real situations.

Fortunately, an analytical solution can be found for a sufficiently small Δ ensuring the condition $L\mathrm{Im}(q) << 1$. In this case, ω and Δ are determined by the conditions $qL = n\pi$ and

$$\Delta = -½\delta\,(n\pi)^2 / (\delta L\tau/4)^3\,, \tag{3}$$

where the integer number n is the edge mode number ($n = 1$ corresponds EM frequency (reflection coefficient minimum) closest to the stop-band edge).

The field distributions corresponding to the EM numbers $n = 1, 2, 3$ are presented in Figure 3. It shows that the EM field is localized inside the CLC layer, and its energy density experiences oscillations inside the layer with the number of the oscillations equal to the EM number n. However, the total field at each point of the CLC layer is represented by two plane waves propagating in the opposite directions [14].

Thus, the intensities of the waves propagating in the opposite directions can be calculated separately at any point in the layer. These distributions are of a special interest close to the layer surfaces. It happens that at the layer surface, the intensity of the wave directed inside the layer is strictly zero, but the intensity of the wave propagating outside the layer is non-zero (although small) [14]. This means that the EM energy is leaking from the layer through its surfaces and the EM life-time τ_m is finite.

For sufficiently thick CLC layers, as the thickness L increases, the EM life-time τ_m (as analytical solution shows [14]) increases as the third power of the thickness, and is inversely proportional to the square of the EM number n. The EM life-time τ_m is given as

$$\tau_\mu = 1/\mathrm{Im}(\omega_{\mathrm{EM}}) = (\mathrm{L/c})\,(\delta\mathrm{L/pn})^2\,. \tag{4}$$

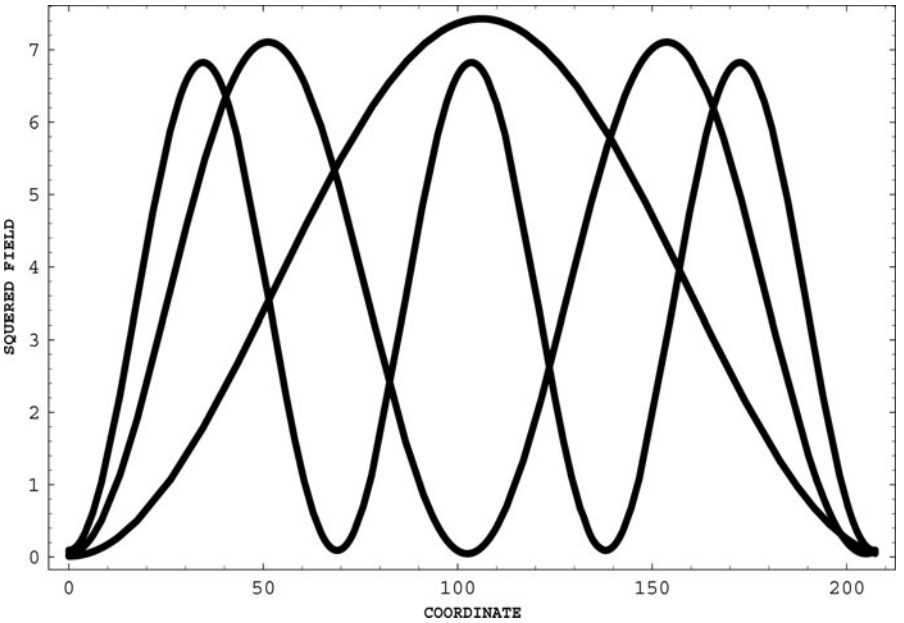

Figure 3. The calculated EM energy (arbitrary units) distributions inside the CLC layer vs. the coordinate (in the dimensionless units $z\tau$) for the three first edge modes ($\delta = 0.05$, $N = 16.5$, $n =$ 1,2,3).

4. Absorbing Liquid Crystal

For the beginning we assume for simplicity that the absorption in the LC is isotropic. We define the ratio of the imaginary part to the real part of the dielectric constant as γ, i.e. $\varepsilon = e_0(1+i\gamma)$. Figure 4 illustrates the 1-*R-T, i.e.* the absorption in the layer, dependence on the frequency for a positive γ, where here R and T are now the intensity reflection

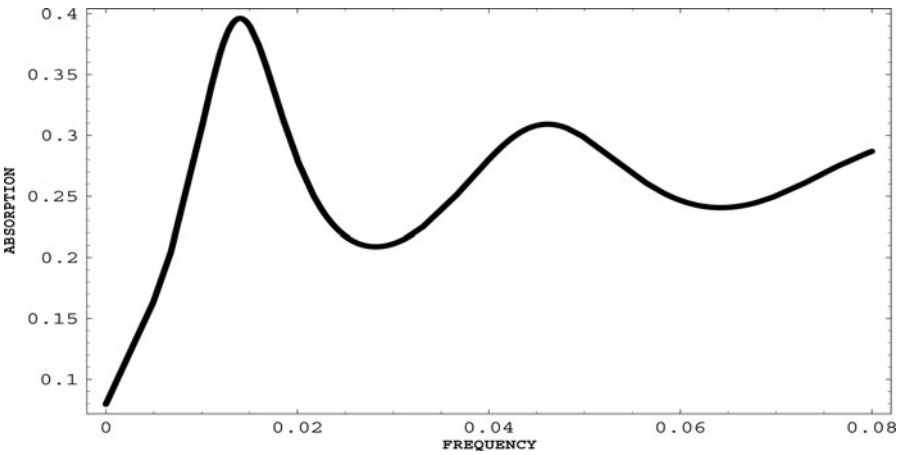

Figure 4. The absorption 1-R-T calculated vs. the dimensionless frequency $\nu = \delta[2(\omega - \omega_B)/(\delta\omega B) -1]$ used also in all figures below, ($l = 300, l = Lt = 4pN$, $\delta = 0.05$) for $\gamma = 0.001$.

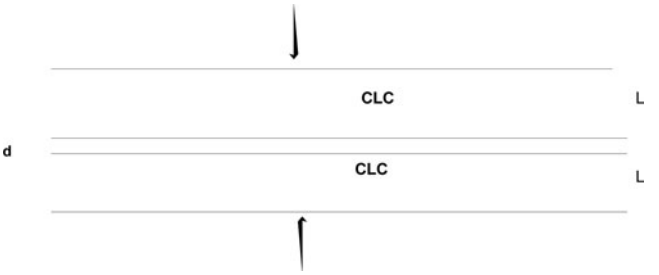

Figure 5. Schematic of the structure with a defect layer (DMS).

and transmission coefficients, respectevely. Now $R+T < 1$. It happens that, for each n, the maximum absorption (i.e. maximal 1-R-T), occurs for

$$(\mathrm{n}\pi)^2 = a^3\,\gamma \tag{5}$$

where $a = \delta L\tau/4$ (in a typical situation, $a >> 1$). From Eq. (5),it follows that the maximum absorption occurs for a special relation between δ, γ and L. As was shown in refs. [11, 15], just at the frequency values determined by Eq. (5), the effect of anomalously strong absorption reveals itself for an absorbing chiral LC (Figure 4).

5. Amplifying Liquid Crystal

We now assume that $\gamma < 0$, which means that the CLC is amplifying. If $|\gamma|$ is sufficiently small, the waves emerging from the layer exist only in the presence of at least one external wave incident on the layer. In this case, $R+T > 1$ (or 1-R-$T < 0$), which just corresponds to the definition of an amplifying medium.

However, if the imaginary part of the dielectric tensor (i.e. γ) reaches some critical negative value, the quantity ($R+T$) diverges and the amplitudes of waves emerging from the layer are nonzero even for zero amplitudes of the incident waves. The corresponding γ is a minimum threshold gain at which the lasing occurs. The equation determining the threshold gain (γ) coincides with Eq. (2). However, it should be solved now not for the frequency but for the imaginary part of the dielectric constant (γ).

For a very small negative imaginary part of the dielectric tensor ($|\gamma|$) and $L|\mathrm{Im}(q)| \ll 1$, the threshold values of the gain for the EM can be represented by analytic expression [14]:

$$\gamma = -\delta\,(n\pi)^2\,/\,(\delta L\tau/4)^3\,. \tag{6}$$

6. Boundary-Value Problem for Defect Mode

The defect mode structure (DMS), which is under consideration here, is shown in Figure 5. The solution to the boundary problem is carried out in the similar way as for a CLC layer above. As such, we give below the final results (all the simplifications assumed above for the CLC layer are implemented for the DMS too).

There is an option to obtain formulas determining the optical properties of the structure depicted in Figure 5 via the solutions found for a single CLC layer [14]. If one uses the expressions for the amplitude transmission $T(L)$ and reflection $R(L)$ coefficients for a single

cholesteric layer (1a) and (1b) (see also[11, 12]), the transmission and reflection intensity coefficients for the whole structure may be presented in the following forms:

$$\mathrm{T(d,\,L)} = \left|\left[\mathrm{T_e T_d}\exp(\mathrm{ikd})\right] / \left[1 - \exp(2\mathrm{ikd})\,\mathrm{R_d R_u}\right]\right|^2 , \tag{7}$$

$$\mathrm{R(d,\,L)} = \left|\left\{\mathrm{R_e} + \mathrm{R_u T_e T_u}\exp(2\mathrm{ikd}) / \left[1 - \exp(2\mathrm{ikd})\,\mathrm{R_d R_u}\right]\right\}\right|^2 , \tag{8}$$

where $R_e(T_e)$, $R_u(T_u)$ and $R_d(T_d)$ (Figure 5) are the amplitude reflection (transmission) coefficients of the CLC layers (Figure 1) for the light incidences on the outer (top) layer surface, the inner top CLC layer surface from the inserted defect layer, and the inner bottom CLC layer surface from the inserted defect layer, respectively. It is assumed in deriving Eqs. (7) and (8) that the external beam is incident on the structure (Figure 5) from the above only.

The calculated reflection spectra inside the stop band for the structure of Figure 5 for non-absorbing CLC layers are presented in Figure 6. The figures show the minima of R at some frequencies inside the stop band at positions which depend on the defect layer thickness d. The corresponding minima of R(d,L) and maxima of T(d,L) happen at frequencies corresponding to the DM frequencies [1–3, 6, 7].

For the layer thickness $d = p/4$, which is just one-half of the dielectric tensor period in a CLC, these maxima and minima are situated just at the stop band center. In the d/p interval $0 < d/p < 0.5$, the value of DM frequency moves from the high frequency stop band edge to the low frequency one. Figure 6 presents only $R(d,L)$ because, for a non-absorbing structure 1 -R(d,L) -T(d,L) = 0. Figure 6 shows that, at some frequency, the reflection coefficient $R(d,l) = 0$. From Eq. (8), one finds that the equation determining the frequencies of the reflection coefficient zeros is presented by the formula:

$$\mathrm{R}_e \left[1 - \exp(2\mathrm{ikd})\mathrm{R_d R_u}\right] + \mathrm{R_u T_e T_u}\exp(2\mathrm{ikd}) = 0. \tag{9}$$

7. Defect Mode

Similarly to the case of EM, the DM frequency ω_D is determined by the zeros of the determinant of the system corresponding to the boundary-value solution for the structure depicted in Figure 5 [16, 17]. The determinant zero value can be explicitly given as

$$\begin{aligned}\{&\exp(2\mathrm{ikd})\sin^2 \mathrm{qL} - \exp(-\mathrm{i}\tau\mathrm{L})\left[(\tau\mathrm{q}/\kappa^2)\cos \mathrm{qL}\right.\\ &\left.+\mathrm{i}\left((\tau/2\kappa)^2 + (\mathrm{q}/\kappa)^2 - 1\right)\sin \mathrm{qL}\right]^2/\delta^2]\} = 0.\end{aligned} \tag{10}$$

It is to be noted that, for a non-absorbing CLC, at a finite length L Eq. (10) does not reach zero for a real value of ω. However, it can reach zero when ω is complex.

Using Eq. (8), the dispersion Eq. (10) may be reduced to the expression containing the amplitude reflection coefficients $R(L)$ of the CLC layers. Thus, one can finally have

$$1 - \mathrm{R(L)_d R(L)_u}\exp(2\mathrm{ikd}) = 0 \tag{11}$$

The field of DM in each CLC layer is a superposition of two CLC eigenmodes [11, 12], and can be easily found. In particular, the coordinate dependence of the squared modulus of the whole field is presented in Figure 7. It shows that, for larger dielectric anisotropy δ, the DM field presents a more sharp growth toward the place where the defect layer occurs.

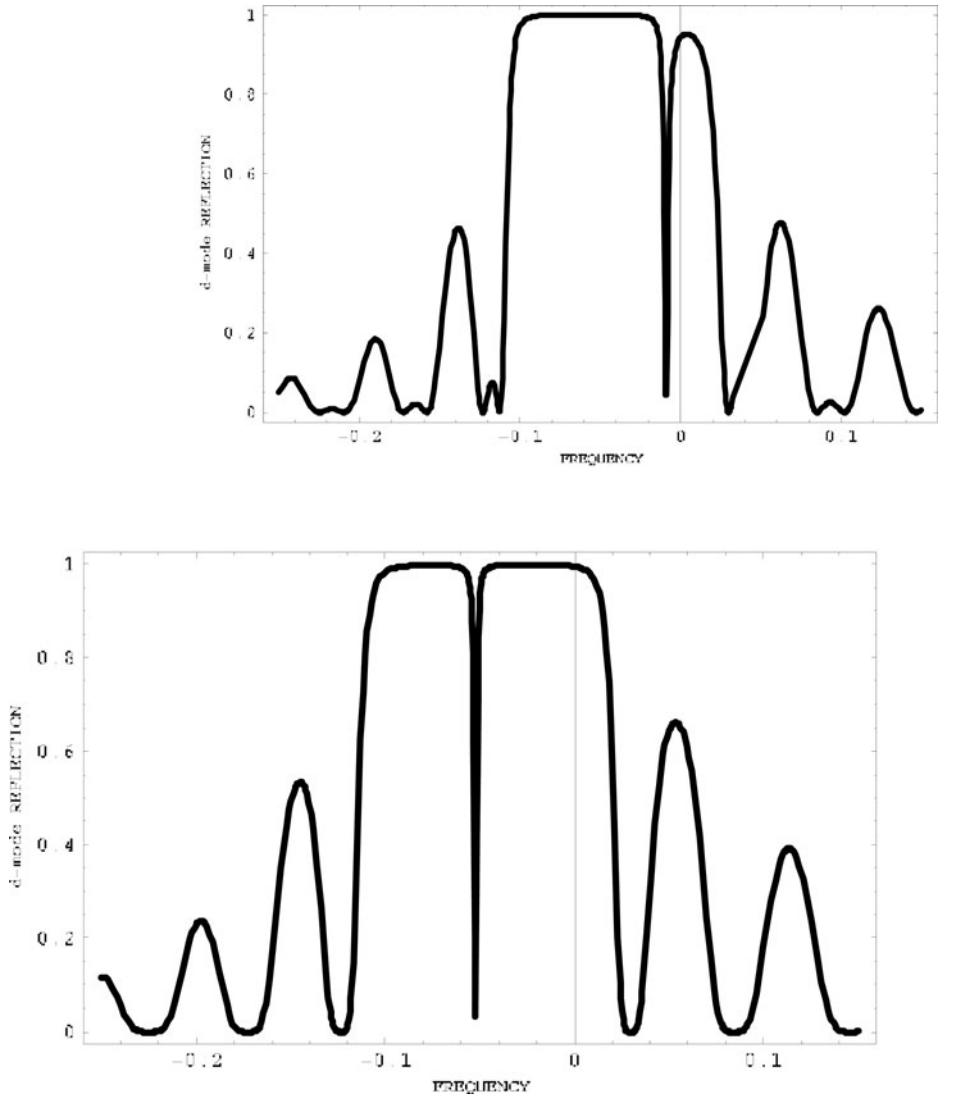

Figure 6. $R(d,L)$ vs. the frequency for a non-absorbing CLC ($\gamma = 0$) at $d/p = 0.1$ (top) and $d/p = 0.25$ (bottom); $\delta = 0.05$, $l = 200$, $l = L\tau = 4\pi N$, where N is the director half-turn number at the CLC layer thickness L.

Similarly to the EM case, at the external surfaces of the DMS, only the amplitude of the wave directed toward the defect layer reduces strictly to zero [16, 17].

The amplitude of the wave directed outwards is small, but does not reduce to zero. This is why there is a leakage of the DM energy outwards through the external surfaces of the DMS. The ratio of the corresponding energy flow to the whole DM energy accumulated in the DMS determines the inverse life-time.

For non-absorbing CLC layers, the only source of decay is the energy leakage through their surfaces. The analysis of the corresponding expressions [16, 17] shows that the DM

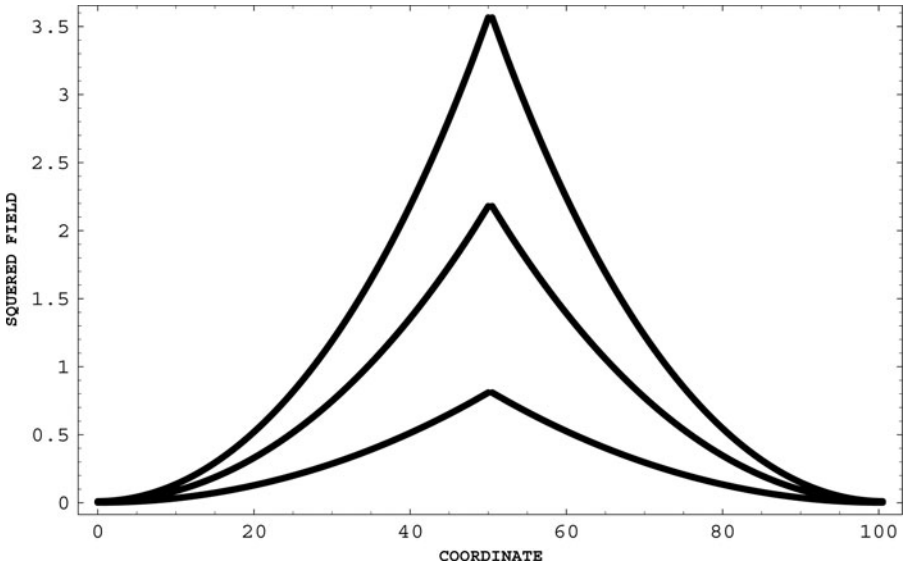

Figure 7. Coordinate dependence of the squared amplitude of the DM field (arbitrary units) at the DM frequency for various dielectric anisotropies (from the top to the bottom d = 0.05, 0.04, 0.025) and the defect layer thickness $\delta = p/4$ for the cholesteric layer thickness $L = 50(p/2)$.

lifetime τ_m is dependent on the position of the DM frequency ω_D inside the stop band, and reaches a maximum just at the middle of the stop band, i.e. at $k = \tau/2$.

8. Thick CLC Layers

In the case of DMS with thick CLC layers ($(|q|L \gg 1)$), some analytical results related to DM can be also obtained similarly as for the EM. In particular, the defect mode life time τ reaches a maximum for the defect mode frequency at the stop band center at fixed CLC layers thickness. For the DM frequency at the middle of the stoop band, i.e. at $k = \tau/2$, the DM life time τ_m is given by

$$\tau_{\mathrm{m}} = \left[(3\pi/c\tau)\,(\mathrm{L/p})\,\epsilon_0^{1/2}\right] \exp\left[2\pi\delta \mathrm{L/p}\right]. \tag{12}$$

Equation (12) reveals an exponential increase of τ_m with increase of the CLC thickness L.

9. Absorbing and Amplifying Liquid Crystals

To take into account the absorption, we again assume $\varepsilon = \mathrm{e}_0(1+i\gamma)$. There are some interesting peculiarities of the optical properties of the structure under consideration (Figure 5). The total absorption at the DM frequency behaves itself unusually. For a small γ, the absorption at the DM frequencies occurs to be much more than the absorption out of the stop band [17]. It is a manifestation of the so-called *anomalously strong absorption effec*t known for perfect CLC layers at the EM frequency [11, 15].

So, at the DM frequency ω_D, one sees that the effect of anomalously strong absorption (similar to the one for EM [11, 15]) exists [16, 17]. Moreover, the absorption enhancement

for DM for small γ is higher than that for EM. In the case of thick CLC layers, the dependence of γ on L and other parameters ensuring maximal absorption may be found analytically. For the position of ω_D just in the middle of the stop band, the expression for γ ensuring maximal absorption takes the following form

$$\gamma = (4/3\pi)(\mathrm{p/L})\exp[-2\pi\delta(\mathrm{L/p})] \tag{13}$$

The results for the transmission and reflection coefficients at $\gamma < 0$ show that, for a small absolute value of γ, the shapes of the transmission and reflection coefficients are qualitatively the same as for zero amplification ($\gamma = 0$). For a growing absolute value of γ, a divergence of R(d,L) and T(d,L) happens at some point [16, 17] with no signs of noticeable maxima at other frequencies. The corresponding value of γ may be considered as close to the threshold value of the gain for the DFB lasing at the DM frequency.

Continuing the increase of the absolute value of γ, one finds that the diverging maxima for R(d,L) at the EM frequencies appear (without traces of maximum at the DM frequency) for the gain being approximately four times more than the threshold gain for the DM [16, 17].

The observed results show that the DM lasing threshold gain is lower than the corresponding threshold for the EM. Another conclusion revealed from this study is the existence of some interconnection between the LC parameters at the lasing threshold, which for thick CLC layers was found analytically for DM (see [16, 17] and Eq. (6) for the EM). A continuous increase of gain results in consequential appearance of lasing at new EM; with the disappearance of lasing at the previous EMs corresponding to lower thresholds (what was experimentally observed [3]).

The mentioned above interconnection between the LC parameters at the lasing threshold in the case of thick CLC layers may be found analytically. If the DM frequency ω_D is located at the stop band center, the corresponding interconnection for the threshold gain (γ) is given by the formula in Eq. (13) with a negative sign on the right-hand-side of the expression. Equation (13) gives that exponentially small value of for thick CLC layers confirms the statement mentioned above about lower lasing threshold for DM compared to EM.

The defect type considered above is a homogenous layer. The developed approach is applicable also to a defect of *phase jump* type [2, 3, 6, 7], and therefore, the corresponding results are practically the same as above. Namely, one gets the equations related to the case of a *phase jump defect* if one performs in the equations presented above a substitution in the factor exp(2ikd), instead of 2*kd*, the quantity $\Delta\varphi$ should be inserted, where $\Delta\varphi$ is the spiral phase jump at the defect plane.

11. Defect Mode with an Active Defect Layer

The DMs studied above are related to isotropic defect layers. Recently a lot of new types of defect layers have been studied [18–24]. The studies performed in [25–28] were limited to a birefringent or absorbing (amplifying) layer inserted in a chiral liquid crystal. The reason for that is connected to the experimental [23, 29] and theoretical [30-32] research on the DFB lasing in CLC where a defect layer is birefringent or absorbing (amplifying) with a general idea that the unusual properties of DM manifest themselves most clearly just at the middle of DMS, i.e. at the defect layer where the intensity of the DM field reaches its maximum. The analytic approach in the study of a DMS with a birefringent or absorbing (amplifying) defect layer is very similar to the previously performed DM studies

for isotropic defect layer [16, 17]. Therefore, we state here the final results of the present investigation with the suggestion to the readers to go through refs. [16, 17] for a detailed approach.

An analytical solution of the DM associated with an insertion of a birefringent or absorbing (amplifying) defect layer in the perfect cholesteric structure was presented for light propagating along the helical axes in [25–28]. The general conclusion of the works [25–28] is that the active layer (excluding an amplifying one) reduces the DM lifetime and increase the lasing threshold in comparison with the case of DM at an isotropic defect layer.

12. Liquid Crystals with Locally Anisotropic Absorption

The discussed above case of isotropic absorption in CLC does not cover all options happening in CLC. For example, quite common is alignment of dye molecules with clearely presented absorption lines in liquid crystals. If the director distribution in a liquid crystal sample is not homogenious (what is the case of CLC) the local anisotropy of absorption in the sample exists and manifests itself in some circumstances [11, 12]. The corresponding effects depend on the value of liquid crystal order parameter and disappeare if the order parameter value is zero, i.e. at the point of liquid crystal phase transition to liquid. The corresponding effects in the transmission and reflection spectra, in particular Borrmann effect, were studied both experimentally [33, 34] and theoretically [11, 12, 33]. In the present section the influence of local anisotropy of absorption on characteristics of localized modes is theoretically studied.

So, let us begin from discussing of the dielectric tensor of a substance with anisotropic absorption. The principal values of corresponding dielectric tensor are complex and have different imaginary parts. In general case all three imaginary parts are different. For simplification of the problem we shall asume that only two principal values of dielectric tensor are complex. Returning to the CLC we assume that the axis corresponding to a real principal value of the dielectric tensor is directed along the spiral axis and two other axes corressponding to complex principal values are rotating around the spiral axis. These rotating axes determine the local depending on the coordinate along spiral axis direction of absorption anisotropy.

It is why now we have to insert two complex principal values of dielectric tensor in the expressions for dielectric anisotropy after formulas (1). As the result the dielectric anysotropy δ becomes a complex quantity. Luckelly, the expressions for reflection and transmission coefficients (1) are exact and are applicable to the case of anisotropic absorption which is under concideration here.

As we expect the local absorption anisotropy reveal itself in DMS reflection and transmission spectra due to the Borrmann effect [11, 12, 33]. Figures 8 and 9 demonstrate Borrmann effect in reflection for a CLC layer and DMS with local absorption anisotropy. Figures 8 and 9 present the calculation results and show that the stop-band edges become nonequivalent in scattering spectra (for no-nabsorbing CLC or CLC with isotropic absorption the reflection is symmetric relative to the stop-band center).

The reflection coefficient value close to the frequencies of one stop-band edge is much more large than close to the frequencies of the other stop-band edge. Figures 10 and 11 demonstrate Borrmann effect in transmission for a CLC layer and DMS with local absorption anisotropy. Figures 10 and 11 show that the stop-band edges are also nonequivalent in transmission spectra.

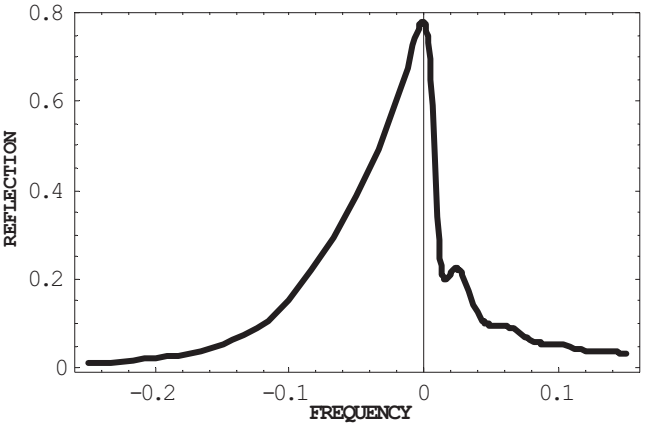

Figure 8. Borrmann effect in reflection for EM (see Fig.1) for locally anisotropic absorption in CLC at $\delta = 0.05 + 0.03i$, N = 300.

The transmission coefficient value close to the frequencies of the same as for the reflection stop-band edge is much larger than close to the frequencies of the other stop-band edge.

Naturally, that the total absorption (1 – R – T) has to be different at the stop-band edges

Figures 12 and 13 demonstrate that due to the Borrmann effect existing in transmission and reflection spectra for a CLC layer and DMS with local absorption anisotropy a suppression of the total absorption occurs at the frequencies close to one of the stop-band edges.

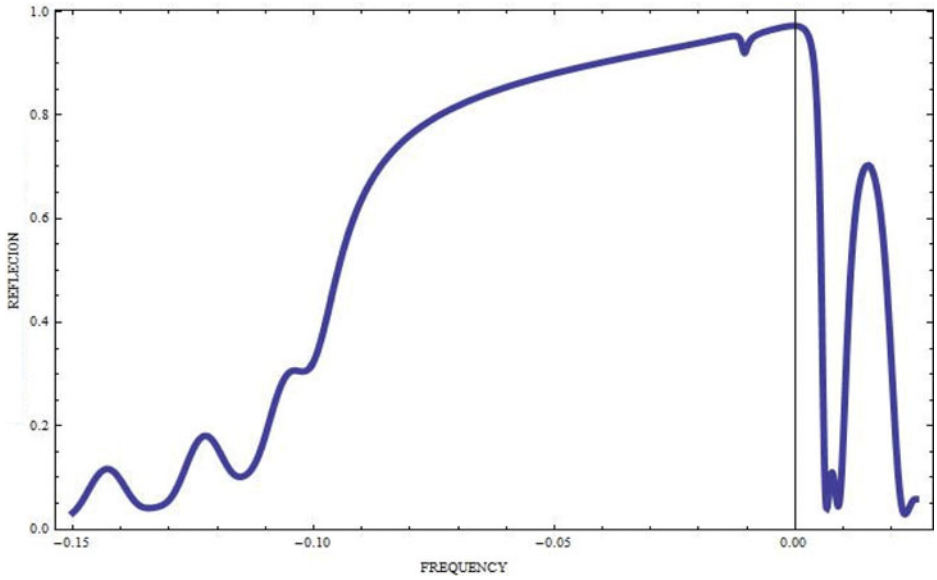

Figure 9. Borrmann effect in reflection for DMS (see Fig. 5) for locally anisotropic absorption in CLC at $\delta = 0.05 + 0.003i$, N = 75, d/p = 0.1.

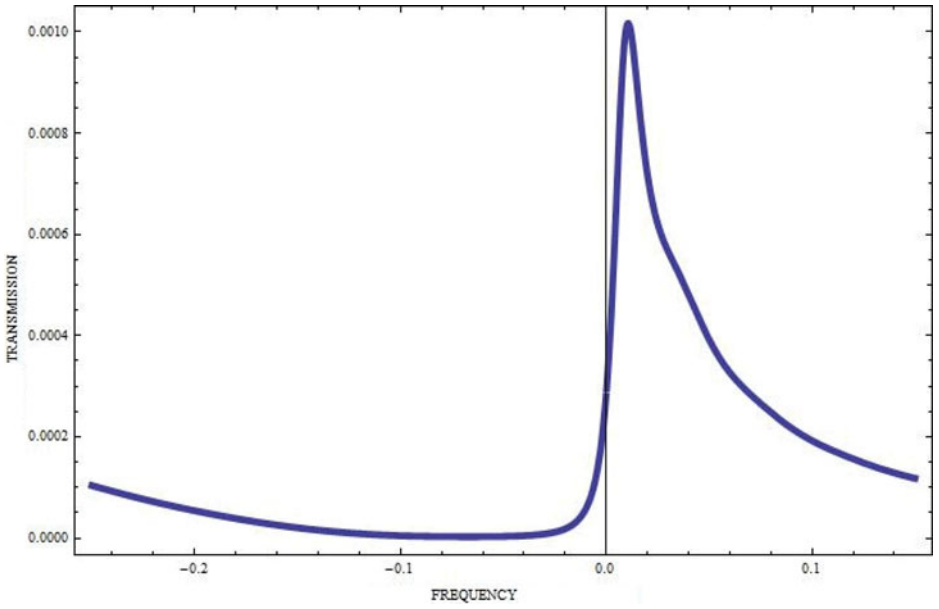

Figure 10. Borrmann effect in transmission for EM for locally anisotropic absorption in CLC at $\delta = 0.05 + 0.015i$, N = 300.

The strength of the discussed effect depends on the order parameter value and the effect disappear for zero order parameter value being at the maximum at its value equal to 1.

The presented reflection and transmission spectra for EM and DM show that the EM and DM life times in the case of a local absorption anisotropy in CLC depends on the

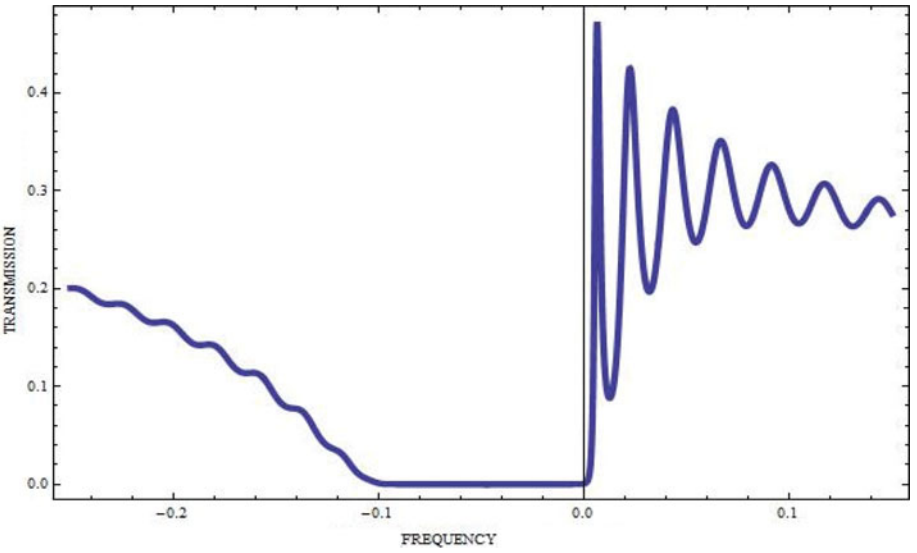

Figure 11. Borrmann effect in transmission for DMS for locally anisotropic absorption in CLC at $\delta = 0.05 + 0.003i$, N = 75, d/p = 0.1.

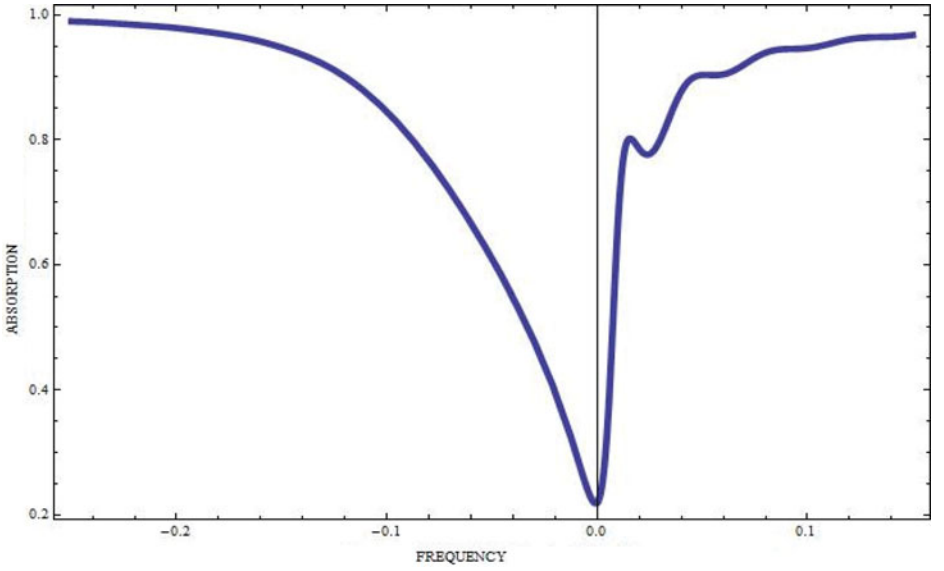

Figure 12. Total absorption in CLC layer for locally anisotropic absorption in CLC at $\delta = 0.05 + 0.015i$, N = 300 (see Fig.1).

localized mode frequency position relative the stop-band edge frequency growing with approach of the localized mode frequency to the stop-band edge frequency where the manifestation of the Borrmann effect takes place. To find the EM and DM life times in the general case one has to solve numerically the dispersion Equations (2) and (10) for EM and DM, respectively. However for sufficiently thick CLC layers an analytical solution may be found.

For example, if the CLC layer thickness L is sufficiently large and the role of inevitably present in real situations isotropic absorption in the determining of the EM life-time exceeds

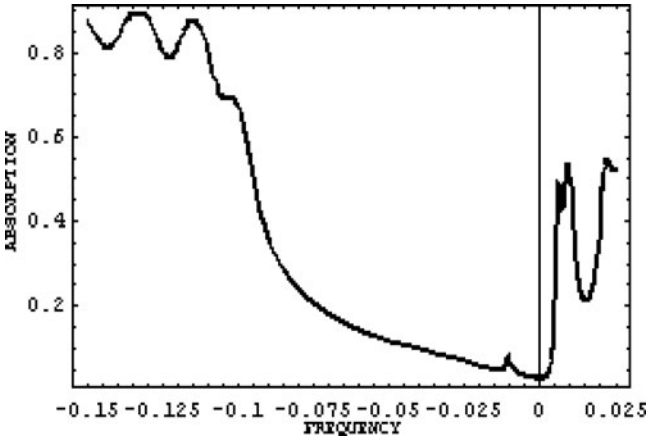

Figure 13. Total absorption in DMS for locally anisotropic absorption in CLC (see Fig. 5) at $\delta = 0.05 + 0.003i$, N = 75, d/p = 0.1.

the role of energy leakage through the layers surfaces the ratio of life-time at the edge frequencies may be estimated by the following expression:

$$\tau_B/\tau_{AB} = \omega_{EM}(\in_0 \gamma + 2 \in_0 \mathrm{Im}\delta + 1/\tau_m)/(\omega_{EM} \in_0 \gamma + 1/\tau_m), \tag{14}$$

where τ_B, τ_{AB}, τ_m are the life-time at the stop-band edge where the Borrmann effect happens, at the opposite edge, at the edges in the case of non-absorbing CLC (see (4)), respectively, and γ is the determining isotropic component of absorption quantity given by the same as above expression $\varepsilon = e_0(1 + i\gamma)$. If γ is approaching zero what is happening when the order parameter is approaching 1 (if we neglect all sources of absorption except the dye) τ_B is coinciding with τ_m given by (4), what corresponds complete suppression of absorption for EM at the stop-band edge frequency in the case of CLC with local anisotropy of absorption. At the opposite stop-band edge frequency the absorption is enhanced and the EM life-time being proportional to $1/2\in_0 \mathrm{Im}\ \delta$ is shorter than τ_m.

13. Conclusion

The performed analytical description of the EM and DM (neglecting the polarization mixing) allows one to reveal clear physical pictures of these modes, which is applicable to the EM and DM in general. For example, lower lasing threshold and stronger absorption at the DM frequency compared to the EM frequencies are the features of any periodic media. Note that the experimental studies of the lasing threshold in ref. [3] agree with the corresponding theoretical results [25–28]. Moreover, the experiment ref. [3] confirms also the existence of some interconnection between the gain and other LC parameters at the threshold pumping energy for lasing at the DM and EM frequencies. For a special choice of the parameters in the experiment, the obtained formulas may be directly applied. However, one has to generally take into account a mutual transformation at the boundaries of the two circular polarizations of opposite sense. In the general case, the EM- and the DM-field leakages from the structure are determined as well by the finite CLC layer thickness. Only for sufficiently thin CLC layers, or in the case of the DM frequency being very close to the stop-band frequency edges, the main contribution to the frequency width of the EM and DM is due to the thickness effect, and the above developed model may be directly applied for describing of the experimental data.

The results related to CLCs with local anisotropy of absorption may be useful for optimizing of DFB lasing. Really, the corresponding theoretical predictions show what one of the two stop-band frequencies is preferable for obtaining the most lower lasing threshold.

An important result related to the DFB lasing at DMS with active defect layer [25–28] may be formulated. The lasing threshold gain in defect layer decreases with the decrease in layer thickness. The similar result relates to the effect of anomalously strong absorption phenomenon where the value of gain in the defect layer (ensuring a maximal absorption) is almost inversely proportional to the defect layer thickness. Note that the obtained results are qualitatively applicable to the corresponding localized electromagnetic modes in any periodic media, and may be regarded as a useful guide in the studies of the localized modes with an active defect layer in general. It should also be mentioned also that the localized DM and EM reveal themselves in an enhancement of some inelastic and nonlinear optical processes in photonic LCs. For examples, the experimentally observed effects for the enhancement of nonlinear optical second harmonic generation [35] and lowering of the lasing threshold [36] in photonic LCs have to be mentioned along with the theoretically predicted enhancement of Cerenkov radiation [11, 12]. Finally, the results obtained here for

the EM and DM (see also [16] and [32]) clarify the physics of these modes, and manifests a complete agreement with the corresponding results of the previous investigations obtained by implementing numerical approach [13].

Funding

The work is supported by the RFBR grants 14-29-07126-ofi_m and 15-02-08757_a.

References

[1] Yang, Y.-C., Kee, C.-S., Kim J.-E., et al.*et al.* (1999). *Phys. Rev. E*, *60*, 6852–6856.
[2] Kopp, V. I. & Genack, A. Z. (2003). *Phys. Rev. Lett.*, *89*, 033901–033905.
[3] Schmidtke, J., Stille, W., & Finkelmann H. (2003). *Phys. Rev. Lett.*, *90*, 083902–083908.
[4] Shibaev, P. V., Kopp, V. I., & Genack, A. Z. (2003). *J. Phys. Chem. B*, *107*, 6961–6968.
[5] Yablonovitch, E., Gmitter, T. J., Meade, R. D., et al.*et al.* (1991). *Phys. Rev. Lett.*, *67*, 3380–3380.
[6] Becchi, M., Ponti, S., Reyes, J. A., & Oldano, C. (2004). *Phys. Rev. B*, *70*, 033103–033118.
[7] Schmidtke, J. & Stille, W. (2003). *Eur. Phys. J.*, *90*, 353–365.
[8] deVries, H. (1951). *Acta Crystallogr.*, *4*, 219–230.
[9] Kats, E. I. (1971). *Zhurn. Eksperim. Teor. Fiziki.* (English translation *JETP*), *32*, 1004–1022.
[10] deGennes, P. G. & Prost, J. (1993). *The Physics of Liquid Crystals*, Clarendon Press: Oxford, UK.
[11] Belyakov, V. A. & Dmitrienko, V. E. (1989). Optics of Chiral Liquid Crystals; In *Soviet Scientific Reviews/Section A: Physics Reviews*. (Ed.) Khalatnikov, I. M. Harwood Academic Publisher: London, UK.
[12] Belyakov, V. A. (1992). *Diffraction Optics of Complex Structured Periodic Media*; Springer Verlag: New York, US; Chapt. 4, 80–139.
[13] Kopp, V. I., Zhang, Z.-Q., & Genack, A. Z. (2003). *Prog. Quantum Electron.*, *27*, 369–451.
[14] Belyakov, V. A. & Semenov, S. V. (2009). *Zhurn. Eksperim. I – Teor. Fiziki.* (English translation *JETP*), *109*, 687–698.
[15] Belyakov, V. A., Gevorgian, A. A., Eritsian, O. S., & Shipov, N. V. (1987). *Zhurn. Tekhn. Fiz.*, *57*, 1418–1418 [*Sov. Phys. Tech. Phys.* 1987, 32, 843-845, English translation]; *Sov. Phys. Crystallogr.* 1988, 33, 337–341.
[16] Belyakov, V. A. (2008). *Mol. Cryst. Liquid Cryst.*, *494*, 127–138; *Ferroelectrics* 2008, 364, 33–39.
[17] Belyakov, V. A. & Semenov, S. V. (2011). *Zhurn. Eksperim. Teor. Fiziki.* (English translation *JETP*), *112*, 694–705.
[18] Arkhipkin, V. G., Gunyakov, V. A., Myslovets, S. A., et al.*et al.* (2011). *Zhurn. Eksperim. Teor. Fiziki.*, *139*, 666–676.
[19] Hodkinson, I. J., Wu, Q. H., Thorn, K. E., Lakhtakia, A., & McCall, M. W. (2000). *Opt. Commun.*, *184*, 57–63.
[20] Wang, F. & Lakhtakia, A. (2005). *Opt. Exp.*, *13*, 7319–7324.
[21] Song, M. H., Ha, N. Y., Amemiya, K., Park, B., Takanishi, Y., Ishikaw, K., Wu, J. W., Nishimura, S., Toyooka, T., & Takezoe, H. (2006). *Adv. Mater.*, *18*, 193–1999.
[22] Yoshida, H., Lee, C. H., Fuji, A., & Ozaki, M. (2006). *Appl. Phys. Lett.*, *89*, 231913–231921.
[23] Yoshida, H., Ozaki, R., Yoshino, K., & Ozaki, M. (2006). *Thin Solid Films*, *509*, 197–202.
[24] Gevorgyan, A. H. & Harutyunyan, M. Z. (2007). *Phys. Rev. E*, *76*, 031701–031711.
[25] Belyakov, V. A. (2012). *Mol. Cryst. Liquid Cryst.*, *559*, 50–59.
[26] Belyakov, V. A. (2012). *Mol. Cryst. Liquid Cryst.*, *559*, 39–44.
[27] Belyakov, V. A. (2013) In *"New Developments in Liquid Crystals and Applications"*, P. K. Choundry, (Ed.), Nova Publishers: New York, Chp. 7, p.199.
[28] Belyakov, V. A. & Semenov, S. V. (2014). *JETP*, *118*, 798.
[29] Song, M. H., Park, B., Takanishi, Y. et al.*et al.* (2005). *Jpn. J. Appl. Phys. 44*, 8165–8171.

[30] Gevorgyan, A. H. (2008). *Opt. Commun.*, *281*, 5097–5105.
[31] Gevorgyan, A. H. & Harutyunyan, M. Z. (2009). *J. Mod. Opt.*, *56*, 1163–1171.
[32] Belyakov, V. A. (2006). *Mol. Cryst. Liquid Cryst.*, *453*, 43–51; *Ferroelectrics* 2006, 344, 163-171.
[33] Chandrasekhar S. (1977). *Liquid Crystals*, Cambridge Unversity Press: Cambridge.
[34] Aronoshodze, S. N., Dmitrienko, V. E., Khoshtariya, D. G., & Chilaya, G. S. (1980). *Pis'ma ZhETF*, *32*, 19.
[35] Shin, K., Hoshi, H., Chang, D., Ishikawa, K., & Takezoe, H. (2002). *Opt. Lett.*, *27*, 128–135.
[36] Matsuhisa, Y., Huang, Y., Zhou Y., et al.*et al.* (2007). *Appl. Phys. Lett.*, *90*, 091114–091121.